

Trajectory Control of a Cart-inverted Pendulum System in the Presence of a Jet Force for an Open Loop Stabilization

Dr. Zakariya Yahya Mohammad, (Lecturer)
Mechanical Eng. Dept.
College of Engineering
University of Mosul, Mosul, Iraq.

Abstract

This paper presents an investigation on the stabilization and the tracking problem of an inverted pendulum-cart system. An open loop subsystem is augmented to the original components which comprises an auxiliary stable pendant pendulum, (P.P.), and a jet force component. The latter is attached firmly to the auxiliary pendulum in such a way to keep the jet force acting in an alignment to this pendulum. The dynamic equations of the system are derived using Lagrange formulation. The jet force locates the inverted pendulum in the up-right position and holds it stable.

A scheme based on model reference and error driven control is proposed to track the system along a pre-specified trajectory, while the inverted pendulum, (I.P.), maintains its up-right position with fairly negligible oscillation. Real-time dynamic simulation is performed and the results of which are presented to illustrate the validity of the proposed approach.

Key words: cart-inverted pendulum system, self erection, tracking, model reference/error driven control.

الخلاصة

يقدم هذا البحث دراسة حول الاستقرارية والتتبع في منظومة بندول معكوس محمول على عربة. وقد أضيفت إلى المكونات الأصلية منظومة ثانوية بدارة مفتوحة مكونة من بندول بندانت المستقر وجزء لتوليد قوة بثق ويرتبط هذا الأخير بثبات إلى البندول المساعد بحيث يحافظ على تأثير قوة البثق باستقامة مع هذا البندول. تم الحصول على المعادلات الديناميكية للمنظومة باستخدام صيغة لاكرينج. تعمل قوة البثق على وضع البندول المعكوس شاقولياً وتحافظ على استقراريته.

في هذه الدراسة تم اقتراح أسلوب للسيطرة اعتماداً على مراجعة النموذج والخطأ وذلك لغرض تتبع المنظومة لمسار معين في حين يحافظ البندول المعكوس على وضعه الشاقولي بتأرجح ضئيل يمكن إهماله. وقد تم إجراء محاكاة للديناميكية في الزمن الحقيقي واستعراض النتائج لإيضاح صلاحية الأسلوب المقترح.

Nomenclature

| | | | |
|---------------------------------------|--|------------------------|---|
| y, \dot{y}, \ddot{y} | Translational position, velocity and acceleration of the cart. | f | System tracking control force. |
| $y_d, \dot{y}_d, \ddot{y}_d$ | Desired position, velocity and acceleration of the cart. | f' | Control force per unit mass. |
| $\theta, \dot{\theta}, \ddot{\theta}$ | Angular position, velocity and acceleration of the I.P. | e, \dot{e}, \ddot{e} | Cart error signals. |
| $\gamma, \dot{\gamma}, \ddot{\gamma}$ | Angular position, velocity and acceleration of the auxiliary P.P. | K_p | Position error gain. |
| y_1, \dot{y}_1 | Horizontal position and velocity of the I.P. at mass center. | K_v | Velocity error signals. |
| z_1, \dot{z}_1 | Vertical position and velocity of the I.P. at mass center. | ω_n | Natural frequency of error dynamics. |
| y_2, \dot{y}_2 | Horizontal position and velocity of the auxiliary P.P. at mass center. | ζ | Damping ratio of error dynamics |
| z_2, \dot{z}_2 | Vertical position and velocity of the auxiliary P.P. at mass center. | M | System mass matrix. |
| T | Total kinetic energy of the system. | C | System damping matrix. |
| T_1 | kinetic energy of the cart. | K | System stiffness matrix. |
| T_2 | kinetic energy of the I.P. | A | State space system matrix. |
| T_3 | kinetic energy of the P.P. | B | State space input matrix. |
| V | Total potential energy of the sys. | s | Laplace operator. |
| L | The Lagrangian. | I | Unit matrix. |
| f_j | Jet force. | M_m | Model total mass. |
| w | Generalized displacement vector. | m | Cart mass. |
| F_{tot} | The generalized total forcing vector. | m_1 | Inverted pendulum mass. |
| f_y | External force affecting the cart. | m_2 | Pendant pendulum mass. |
| τ_y | Total force affecting the cart. | B_1 | Cart viscous frictional coefficient. |
| τ_θ | Total moment affecting the I.P. | B_2 | I.P. viscous frictional moment coefficient. |
| τ_γ | Total moment affecting the P.P. | B_3 | P.P. viscous frictional moment coefficient. |

| | | | |
|-------------------------|--|-----------|---|
| \dot{y}_m, \ddot{y}_m | Model translational velocity and acceleration. | I_1 | I.P. moment of inertia about the lower pivoted end. |
| $l_1 = 2b$ | Length of the I.P. | I_2 | P.P. moment of inertia about the pivoted end. |
| $l_2 = 2c$ | Length of the P.P. | λ | Eigen values. |

1. Introduction

The stabilization and control of a cart-inverted pendulum system has been considered as a challenging objective in many experimental and theoretical investigations. Many research works are focused on the problem, reach to idea that it is a suitable system on which various control techniques can be examined including non-linear and linear control approaches [1,2,3]. However, other research works treated the problem in conjunction to the application, both theoretically and experimentally. The inverted pendulum have found various application motivating a new field concerning the applied dynamics and control. The application ranges from mobile robots, [4,5], guidance of space rockets [6], structural dynamics during earth quick [7], balancing of a segway which is, simply, a two-wheeled mobile inverted pendulum vehicle, [8], etc. As a new and important application of the stabilization of the inverted pendulum system, in motion, is the convertible four-two wheel chair for disabled person [9]. Different control techniques have been employed to the problem of stabilization and motion tracking of an inverted pendulum system. These are ranging from applying techniques such as PD and optimal control methods to the use of a modern control strategies [2,10,11]. A PD based control was applied for self erecting the pendulum in vertical-upright position, while a linear quadratic regulator was adopted to balance the pendulum [2]. Modern control method using fuzzy controller was used to guarantee the stability of the inverted pendulum after swinging it by a control voltage applied to the motor driving the cart [10].

Reference compensation technique scheme was used as a neural net work control method for a mobile inverted pendulum where experiments are conducted to examine the control performance of both balancing and tracking a desired trajectory [11]. In all of these works, they used a horizontal control forcing to swing-up and balance the inverted pendulum and, or to track the system on some desired trajectory. As an exception, an attempt has been made to use vertical control forcing in order to balance an inverted pendulum system, which is described as a novel approach where a PD controller is designed to satisfy the stability condition, and the proposed hybrid fuzzy control scheme provides a more flexible way to stabilize the inverted pendulum via vertical force. [12]. In the present work, a new and different method for up-right positioning and stabilizing an inverted pendulum with cart trajectory control has been developed and examined by numerical experiments using Matlab/Simulink. Tracking effects of the cart on the inverted pendulum verticality and stability have been examined by performing dynamic simulation in the presence of the stabilizing jet force. A schematic description of the proposed system is shown in figure (1) and the details of the system mathematical modeling and control are as follow;

2. The proposed cart-inverted pendulum system

The cart-inverted pendulum system proposed in this investigation is new and different from the conventional system treated in many previous works. An auxiliary, relatively, light pendant pendulum is hinged freely at the tip of the inverted pendulum. A jet force component aligned, firmly, to the auxiliary pendulum such that, the direction of the induced jet force is, always, acting downward along the pendant pendulum. This force can bring the I.P. from an initial position to the up-right position. The cart on which the inverted pendulum sub-system is supported can move horizontally on some desired trajectory by the application of horizontal force independent on that induced by the jet. A schematic description of the system is given in figure (1). In the proposed system, one concern is the up-right positioning of the inverted pendulum based, firstly, on the non-linear system dynamics. In addition, the performance of the whole system, including the angular position and velocities of the two pendulum, are to be monitored in the presence of a trajectory control of the cart.

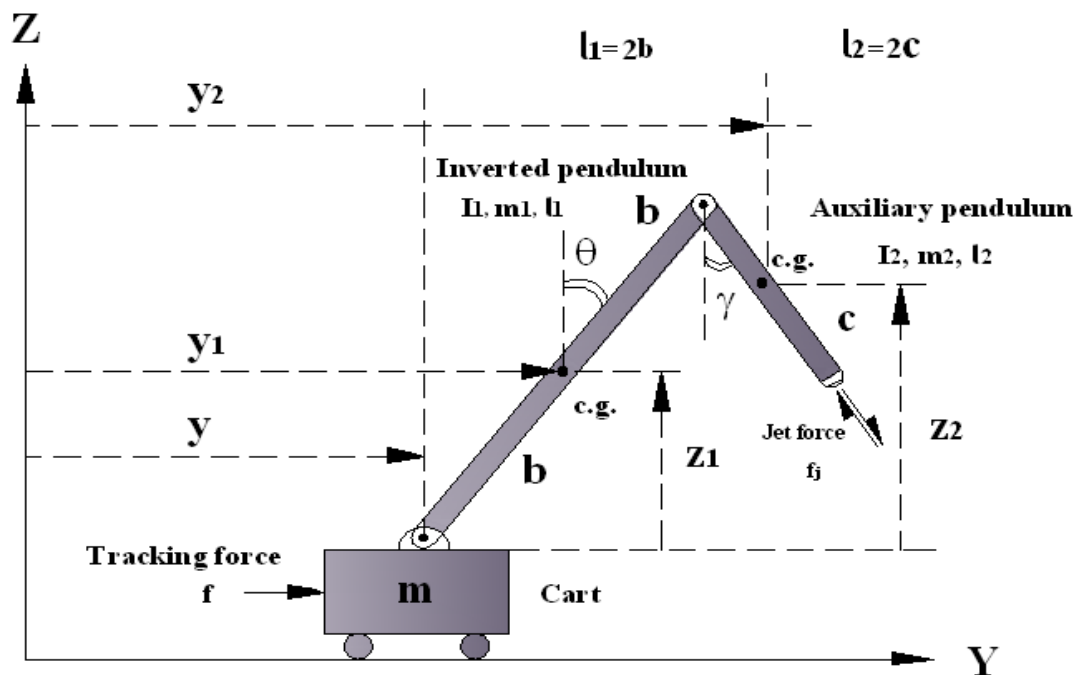


Figure (1): Description of the cart-inverted pendulum system.

1

3. Mathematical Modeling of the system

The modeling of the system is presented. This gives the dynamical equations on which the simulation of the system performance is based. The performance includes that just prior to the application of the trajectory control and in the presence of the trajectory control.

Lagrange formulation is utilized in developing and characterizing the dynamic model of the system, [13,14]. By considering a plane motion, figure (1), the total kinetic energy of the system is due to the translational and rotational motions of the masses, giving :

$$T = T_1 + T_2 + T_3 \tag{1}$$

where: $T_1 = \frac{1}{2}m\dot{y}^2$, $T_2 = \frac{1}{2}m_1(\dot{y}_1^2 + \dot{z}_1^2) + \frac{1}{2}I_1\dot{\theta}^2$ and $T_3 = \frac{1}{2}m_2(\dot{y}_2^2 + \dot{z}_2^2) + \frac{1}{2}I_2\dot{\gamma}^2$

upon substituting ($y_1, \dot{y}_1, z_1, \dot{z}_1, z_2,$ and \dot{z}_2) using the geometry shown in figure (1), where; $y_1 - y = b \sin \theta$, $z_1 = b \cos \theta$, $y_2 - y = l_1 \sin \theta + c \sin \gamma$, $z_2 = l_1 \cos \theta + c \cos \gamma$, the total kinetic and potential energies of the systems in terms of variables ($y, \theta,$ and γ) and their derivatives are obtained as, [14]. The kinetic energy of the system, from equation (1), becomes;

$$T = \frac{1}{2}(m + m_1 + m_2)\dot{y}^2 + \left(\frac{l_1^2}{2}m_2 + \frac{I_1}{2}\right)\dot{\theta}^2 + \left(\frac{I_2}{2}\right)\dot{\gamma}^2 + (m_1b + m_2l_1)(\cos \theta)\dot{y}\dot{\theta} + l_1cm_2 \cos(\theta + \gamma)\dot{\theta}\dot{\gamma} + m_2c(\cos \gamma)\dot{y}\dot{\gamma} \tag{2}$$

And the potential energy of the system is:

$$V = m_1gz_1 + m_2gz_2 = (m_1gb + m_2gl_1)\cos \theta - m_2gc \cos \gamma \tag{3}$$

In order to have a closed form dynamic model of this inverted pendulum-cart system, the energy expression in (2) and (3) are used to establish the Lagrangian; [13,14]

$$L = T - V \tag{4}$$

Upon selecting the generalized displacement vector as:

$$w = [y \ \theta \ \gamma]^T$$

The corresponding generalized total forcing is the following vector;

$$F_{tot} = [\tau_y \ \tau_\theta \ \tau_\gamma]^T$$

Thus the following set of equations based on the Lagrangian formulation are obtained:

$$\left. \begin{aligned} \frac{d}{dt}\left(\frac{\partial L}{\partial \dot{y}}\right) - \frac{\partial L}{\partial y} &= \tau_y = f_y - f_j \sin \gamma \\ \frac{d}{dt}\left(\frac{\partial L}{\partial \dot{\theta}}\right) - \frac{\partial L}{\partial \theta} &= \tau_\theta = -f_j l_1 \sin(\theta + \gamma) \\ \frac{d}{dt}\left(\frac{\partial L}{\partial \dot{\gamma}}\right) - \frac{\partial L}{\partial \gamma} &= \tau_\gamma = 0 \end{aligned} \right\} \tag{5}$$

Here, f_y is the external actuating force applied to the cart .

By return to figure (1) and using equations 2, 3, 4 and 5, and allowing for the effects of damping, drag forces and torque on the system components, the following non-linear dynamical equations are obtained after some manipulation;

$$\left. \begin{aligned}
 (m + m_1 + m_2)\ddot{y} + [(m_1b + m_2l_1)\cos\theta]\ddot{\theta} + (m_2c \cos\gamma)\ddot{\gamma} - [(m_1b + m_2l_1)\sin\theta\dot{\theta}]\dot{\theta} \\
 + B_1\dot{y} - [m_2c \sin\gamma\dot{\gamma}]\dot{\gamma} = f_y - f_j \sin\gamma \\
 [(m_1b + m_2l_1)\cos\theta]\ddot{y} + [l_1^2m_2 + I_1]\ddot{\theta} + [l_1cm_2 \cos(\theta + \gamma)]\ddot{\gamma} - [(l_1cm_2)\sin(\theta + \gamma)]\dot{\gamma}\dot{\theta} \\
 + B_2\dot{\theta} = [m_1gb + m_2gl_1]\sin\theta - f_jl_1 \sin(\theta + \gamma) \\
 [m_2c \cos\gamma]\ddot{y} + [l_1cm_2 \cos(\theta + \gamma)]\ddot{\theta} + I_2\ddot{\gamma} + B_3\dot{\gamma} = -m_2gc \sin\gamma
 \end{aligned} \right\} (6)$$

The above non-linear dynamical equations are linearized and rearranged. The linearization is obtained by assuming small values of angular position changes about the nominal up-right position of the inverted pendulum and the auxiliary pendant pendulum, hence the following approximations may be used:

$$\begin{aligned}
 \theta \approx \sin\theta, \quad \cos\theta \approx 1, \quad (\dot{\theta})^2 \approx 0, \\
 \gamma \approx \sin\gamma, \quad \cos\gamma \approx 1, \quad (\dot{\gamma})^2 \approx 0
 \end{aligned}$$

Equations (6) may be rewritten after linearization in a compact form to obtain;

$$M\ddot{w} + C\dot{w} + Kw = F \tag{7}$$

Where, w and F are the position and forcing vectors respectively, and;

$$M = \begin{bmatrix} (m + m_1 + m_2) & (m_1b + m_2l_1) & m_2c \\ (m_1b + m_2l_1) & (l_1^2m_2 + I_1) & l_1cm_2 \\ m_2c & l_1cm_2 & I_2 \end{bmatrix}, \quad C = \begin{bmatrix} B_1 & 0 & 0 \\ 0 & B_2 & 0 \\ 0 & 0 & B_3 \end{bmatrix}$$

$$K = \begin{bmatrix} 0 & 0 & f_j \\ 0 & (f_jl_1 - m_1gb - m_2gl_1) & f_jl_1 \\ 0 & 0 & m_2gc \end{bmatrix}, \quad w = [y \quad \theta \quad \gamma]^T$$

$$F = [f_y \quad 0 \quad 0]^T$$

Here, (f_y) is the unique external force that is acting on the cart.

4. Trajectory control of the system

In practice, it is normally required not only to bring the I.P. to a stable up-right position, but rather to control the position of the system, so that, it restore it's original position or, it follows a desired trajectory of some specified function of time. [2,10,11]

For this purpose a scheme based on model reference error driven control is adopted. Assuming that a complete description of the desired trajectory and its first two derivatives are available, namely the cart desired position, velocity and acceleration (y_d , \dot{y}_d and \ddot{y}_d) respectively. The dynamics of the reference model is concerned with the translational motion of the system as we have a tracking problem.

The inherent dynamical effects of the rotational elements on a trajectory tracking were ignored. This approximation simplifies the system for the purpose of tracking to be of an equivalent total mass, ($M_m = m + m_1 + m_2$), which is subjected to a viscous damping, including drag force, affecting the cart. Thus, the dynamics of the reference model reduces to the following single degree of freedom system;

$$M_m \ddot{y}_m + B_1 \dot{y}_m = f \tag{8}$$

It is to be mentioned that the best dynamical data for the model are those available from the original system, namely, the cart motion variables (y , \dot{y} and \ddot{y}), so that, equation (8) can be rewritten as:

$$M_m \ddot{y} + B_1 \dot{y} = f \tag{9}$$

A control law is adopted that when it's combined with motion equations it yields a closed loop system. This trajectory control law can be stated as: [15,16]

$$u = \ddot{y}_d + K_v(\dot{y}_d - \dot{y}) + K_p(y_d - y) \tag{10}$$

To establish a control law for this system, we will consider the tracking control of the model stated earlier. A control law partitioning technique is used to reduce the system to a unit mass problem. Further, it is required to decompose the controller into two segments. The first is model based in which the system model parameters are used to set up a control law, such that it reduces the system model to appear as if it is a unit mass.

The second segment of the control law is error driven. Error signal are obtained by differencing desired and actual variables. These error signal are multiplied by a suitable values of gains. These gains are specified according to the required error signal suppression in the sense of its magnitude and duration as will be shown. The model-based portion of the control law takes the form:

$$f = \alpha f' + \beta \tag{11}$$

Where α and β are functions or constants and are to be chosen so that (f') is taken as a new forcing input. Combination of equations (9) and (11), using this structure of control law, gives the following system equation:

$$M_m \ddot{y} + B_1 \dot{y} = \alpha f' + \beta \tag{12}$$

Choosing α and β as ($\alpha = M_m$) and ($\beta = B_1\dot{y}$), results the following unit mass equation:

$$\ddot{y} = f' \tag{13}$$

In the trajectory control system, the error driven portion determines (f') as function of position and velocity errors in away similar to that stated in equation (10). Thus;

$$f' = \ddot{y}_d + K_v\dot{e} + K_p e \tag{14}$$

Substituting for equation (13) in (14), an equation of motion written in error space is obtained as:

$$\ddot{e} + K_v\dot{e} + K_p e = 0 \tag{15}$$

The above error dynamic equation characterizes the amount of error suppression which can be determined by the choice of (K_p) and (K_v) values. A proper choice of gains (K_p) and (K_v) should be that by which errors are suppressed in fastest possible manner with little overshoot. Equation (15) gives the following characteristic equation:

$$s^2 + K_v s + K_p = 0 \tag{16}$$

where ($K_v = 2\zeta\omega_n$), and ($K_p = \omega_n^2$).

The relationship between (K_v) and (K_p) may be obtained to be:

$$K_v^2 = 4\zeta^2 K_p \tag{17}$$

Upon specifying the values of (ζ) and (K_p), (K_v) may be determined. The general form describing this control scheme is shown in figure (2).

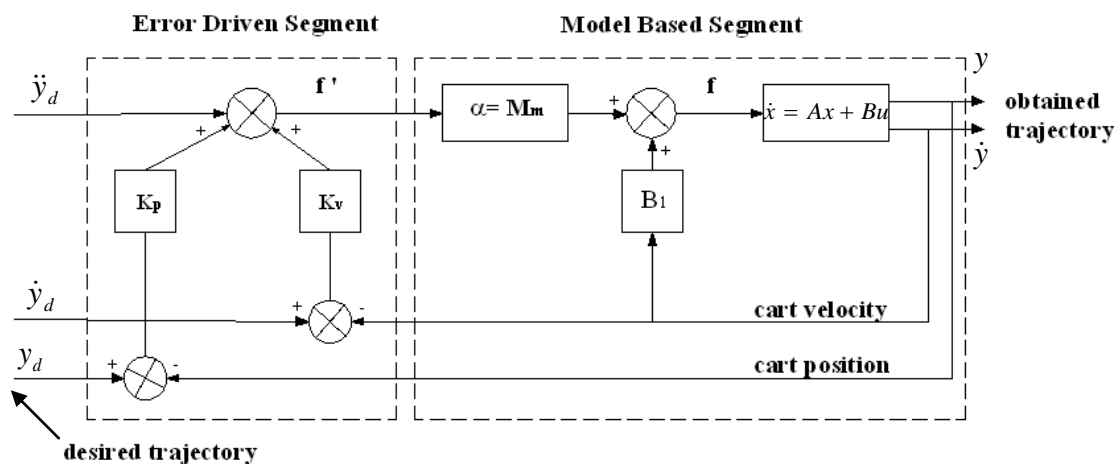


Figure (2): Block diagram of the trajectory control scheme.

5. Simulation of the system dynamics and control

Starting by equation (7), a state space representation of the system can be obtained. Pre-multiplying by (M^{-1}) and rearranging, the following vector-matrix equation is obtained:

$$\ddot{w} = -M^{-1}C\dot{w} - M^{-1}Kw + M^{-1}F \tag{18}$$

Equation (18) may be rewritten in the state space form: $\dot{x} = Ax + Bu$. Hence, a set of partitioned vector-matrix equations are obtained as;

$$\begin{bmatrix} \dot{y} \\ \dot{\theta} \\ \dot{\gamma} \\ \ddot{y} \\ \ddot{\theta} \\ \ddot{\gamma} \end{bmatrix} = \begin{bmatrix} 0 & I \\ -M^{-1}K & -M^{-1}C \end{bmatrix} \begin{bmatrix} y \\ \theta \\ \gamma \\ \dot{y} \\ \dot{\theta} \\ \dot{\gamma} \end{bmatrix} + \begin{bmatrix} 0 & 0 & 0 \\ 0 & 0 & 0 \\ 0 & 0 & 0 \\ M^{-1} & & \end{bmatrix} \begin{bmatrix} f_y \\ 0 \\ 0 \end{bmatrix} \tag{19}$$

With reference to equations (6) and (7), it may be noticed that the above open-loop dynamic system is made asymptotically stable by introducing the jet force parameter (f_j) in the system dynamics, in the manner explained earlier. The only single condition is that the term; $f_j l_1 - m_1 g b - m_2 g l_1$, has to be positive, giving; $f_j > \frac{m_1 g b + m_2 g l_1}{l_1}$, or $(f_j) > 1.57$ N) for a system with parameters given in table (1). Here, the jet force (f_j) has been taken as (2) N.

Table (1): Basic system parameters

| m kg | m_1 kg | m_2 kg | B_1 Ns/m | B_2 Nms/rad | B_3 Nms/rad | g m/sec ² |
|------------|-------------|-------------|---------------|------------------|---------------------------|---------------------------|
| 1 | 0.2 | 0.06 | 0.18 | 0.16 | 0.06 | 9.81 |
| l_1 m | l_2 m | b m | c m | f_j N | I_1 kgm ² | I_2 kgm ² |
| 0.5 | 0.12 | 0.25 | 0.06 | 2 | 1.66x10 ⁻² | 2.88x10 ⁻⁴ |

Using the parameters in table (1), the open loop system and input matrices are obtained as:

$$A = \begin{bmatrix} 0 & 0 & 0 & 1 & 0 & 0 \\ 0 & 0 & 0 & 0 & 1 & 0 \\ 0 & 0 & 0 & 0 & 0 & 1 \\ 0 & 0.575 & 0.604 & -0.1709 & 0.4279 & -0.2907 \\ 0 & -12.161 & -39.87 & 0.4814 & -9.042 & 19.186 \\ 0 & 68.814 & 119.011 & -0.8721 & 51.163 & -324.6124 \end{bmatrix},$$

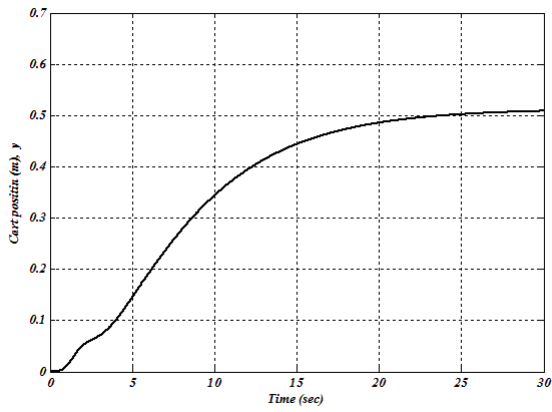
$$B = \begin{bmatrix} 0 & 0 & 0 \\ 0 & 0 & 0 \\ 0 & 0 & 0 \\ 0.9 & -2.7 & 4.8 \\ -2.7 & 56.5 & -319.8 \\ 4.8 & -319.8 & 5410.2 \end{bmatrix}$$

The roots of the open-loop system characteristic reflects the stability condition of the system, obtained as eigen values (λ_i) of the open-loop system matrix, (equation 19). Using the following equation; $|\lambda I - A| = 0$, the eigen values of (A) at ($f_j = 0$), and at ($f_j = 2$ N) are evaluated to be: (0, -327.16, -9.137, 3.2, -0.59, -0.143) with one positive real root causing instability, and (0, -328, $-2.58 \pm i1.36$, -0.42, -0.19) respectively. Clearly, the latter has non-positive sign in all real parts indicating a stable condition. The zero eigen value refers to the cart mass being a damped motion rigid body.

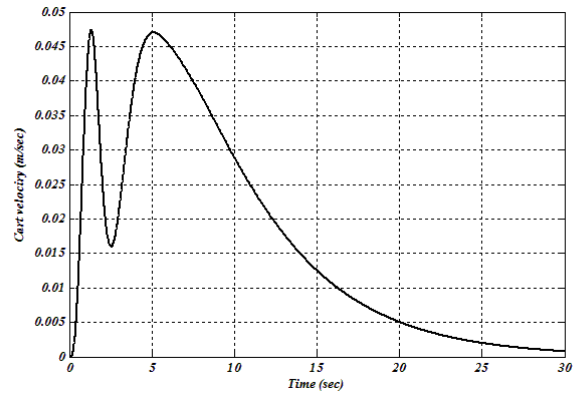
5-1. Up-right localization of the inverted pendulum

The system non-linear dynamical, equations (6), developed earlier with parameters specified in table (1) have been used in establishing Matlab-Simulink simulation block diagram, so that a large initial angle of the inverted pendulum may be used, reflecting a more realistic case. The unforced system, ($f_y = 0$), with an initial angle of the inverted pendulum ($\theta_o = \pi/2$), describing the case of a horizontally positioned I.P., was used to show the effectiveness of using jet force to reach a stable up-right position of the I.P. Upon performing the simulation, the system response represented by positions (y, θ, γ) and velocities ($\dot{y}, \dot{\theta}, \dot{\gamma}$) are shown in figures (3-5).

The I.P., almost, attains the vertical position in about (4 sec.). The following values were noticed; ($\theta=0.05$ rad., $y=0.12$ m, $\gamma=-0.008$ rad, $\dot{\theta} = 0.002$ rad/sec, $\dot{y} = 0.043$ m/sec, $\dot{\gamma} = 0.006$ rad/sec). It may be noticed that the whole system is settled within 20 seconds.

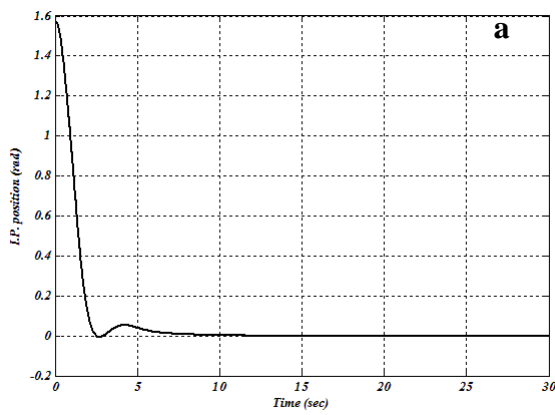


a- Cart translational response

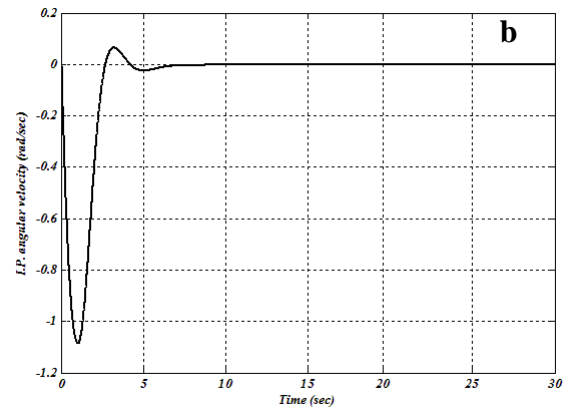


b- Cart translational velocity.

Figure (3)

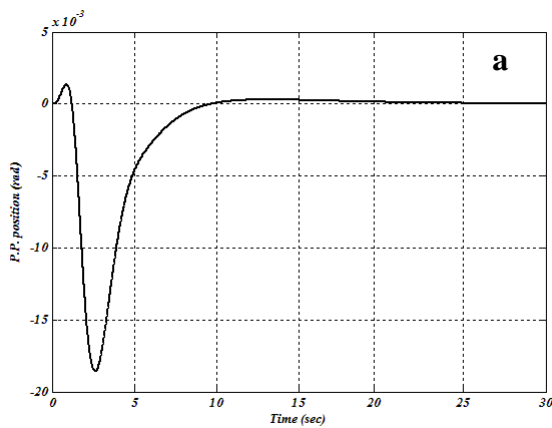


a- Inverted Pendulum angular posion.

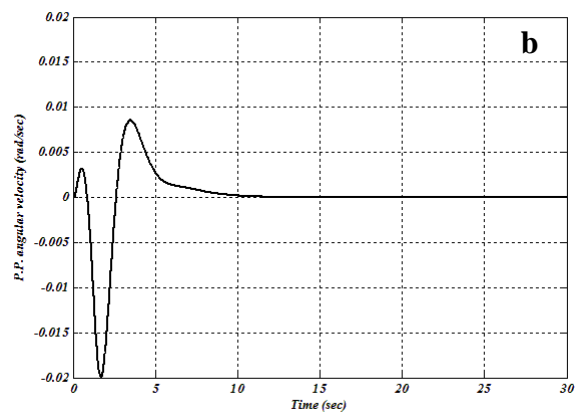


b- Inverted pendulum angular velocity.

Figure (4)



a- Pendant Pendulum angular posion.



b- Pendant pendulum angular velocity.

Figure (5)

5-2. Results of the trajectory control

This section illustrates the behavior of the proposed trajectory control scheme, shown in figure (2). A Matlab program was written to simulate the control system performance. The present controller is activated when the inverted pendulum, almost, attains its up-right position. A piece wise time function trajectory of three segments each with (10 sec) duration were taken as the desired trajectory, y_d . This comprises a parabolic, flat and down ramp shaped functions respectively to reflect an accelerated movement up to (2 m) of cart position, stand still, and a constant speed return to the initial position. Having specified the desired trajectory (y_d), the control scheme described earlier is simulated in which the cart external force (f_y) of equation (19) is to be replaced by the tracking force (f), which is determined in equations (11-14) as;

$$f = B_1\dot{y} + M_m[\ddot{y}_d + k_v(\dot{y}_d - \dot{y}) + k_p(y_d - y)] \quad (20)$$

In matrix state-space notation which is required in the simulation, the feed back system and the input matrices become, respectively, as follow:

$$[A - B \times G], \quad \text{and} \quad [B]$$

where the feed back gain matrix is :

$$G = \begin{bmatrix} (M_m K_p) & 0 & 0 & (M_m K_v - B_1) & 0 & 0 \\ 0 & 0 & 0 & 0 & 0 & 0 \\ 0 & 0 & 0 & 0 & 0 & 0 \end{bmatrix},$$

Here $M_m K_p = 2.52$ and $M_m K_v - B_1 = 3.046$

The corresponding control input is the following vector:

$$U = [u \quad 0 \quad 0]^T$$

Where $u = M_m (K_p y_d + K_v \dot{y}_d + \ddot{y}_d)$ (21)

In the error driven segment and using equation (17), the gain (K_v) was evaluated to be (2.56) after selecting ($K_p = 2$), and ($\zeta = 0.9$). These are chosen for reasonably fast response with very small over shoot in error signal (e), in addition to a reasonable magnitude of actuating force, as this force is directly proportional to the values of gains, K_p and K_v , equation (21). The overall behavior of the system are illustrated in figures (6-8), with initial values of states as obtained earlier, from the results of the non-linear model of the system after 4 sec. Of particular interest are figures (6) of the I.P. angular position (θ) and figures (7-8) of the cart trajectory control results which illustrates a comparison between the obtained and the desired trajectories.

Although, initial values of states were used in the simulation, the inverted pendulum was brought it's up right position in (1.5 sec). However, transient angular deflection of about (0.1 rad.)(5.8°) in maximum is noticed due to disturbances caused by the sudden change in the desired trajectory function. Variations of the pendant pendulum position were found to be very small, figure (9). The cart tracks the desired trajectory very well with a maximum transient error of about (5.5%).

The error signal, figure (10) shows a transient variation of about (0.11 m) in maximum around zero. Finally, the total tracking force is shown in figure (11). This is, in fact, dependent on the selective gains (K_p) and (K_v) as well as the cart drag force. The system closed loop eigen values or poles are obtained to be the following; (-328, -4.13, -1.29 ± i 1.21, -1.43, -0.51). Having obtained the numerical simulation results, the following remarks may be highlighted:

- The jet force (f_j) has a stiffening effect on the I.P.
- The values of (K_p) and (K_v), indirectly, affect the system states other than those of the cart.
- It seems that the error induced using simplified reference model is embedded within the major tracking error signal forming a collective error which drives the tracking controller.
- The present scheme shows some kind of robustness as errors in estimating model mass (M_m) will, effectively, be reflected on the assigned values of gains (K_p) and (K_v) which are not critical. This may be noticed by an insite look to the structure of the trajectory control block diagram, figure (2).
- A compromise between the fastness and accuracy of the tracking response with the magnitude of the tracking forces has to be made in determining the gains values (K_p) and (K_v). The higher the gain values, the larger will be the required tracking force.

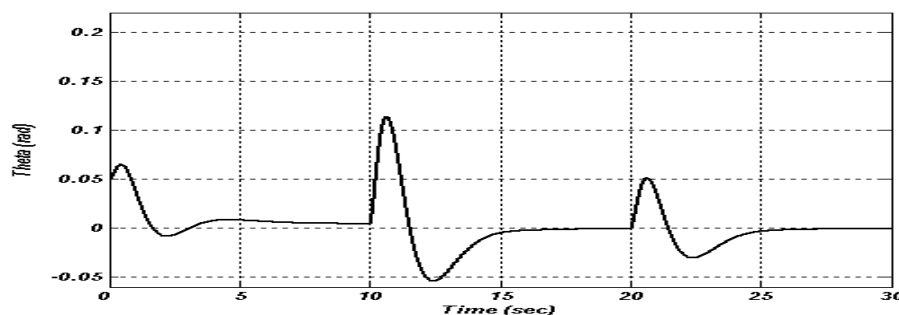


Figure (6): I.P. angular position during tracking.

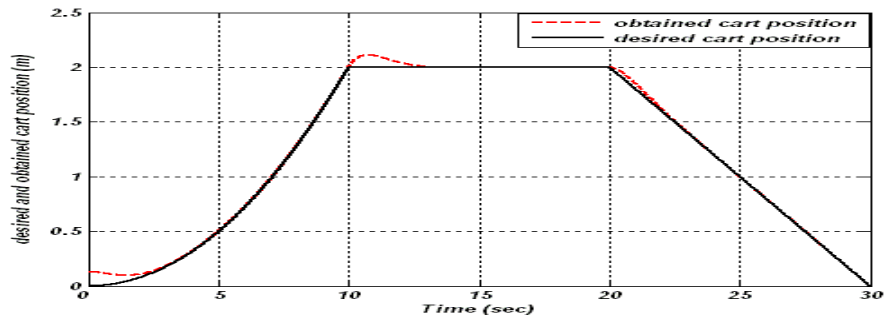


Figure (7): Desired and the obtained cart position during tracking.

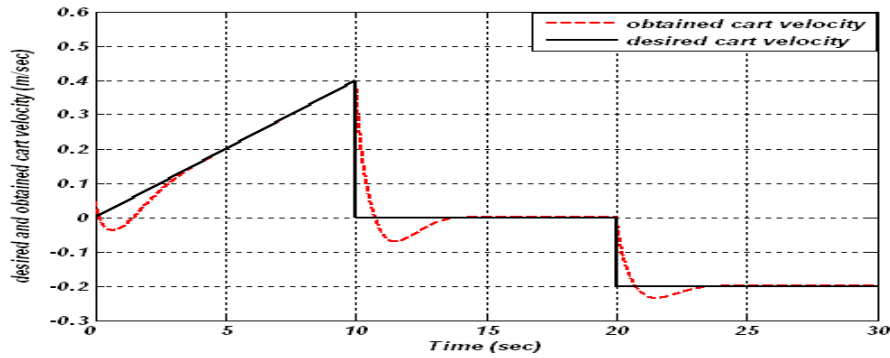


Figure (8): Desired and the obtained cart velocity during tracking

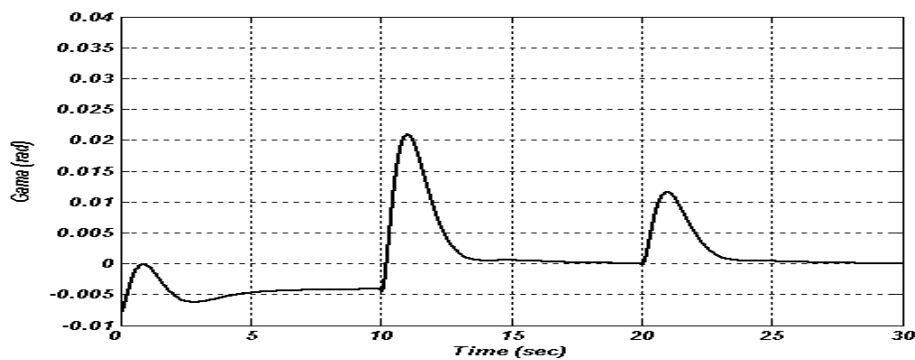


Figure (9): Pendant pendulum angular position during tracking

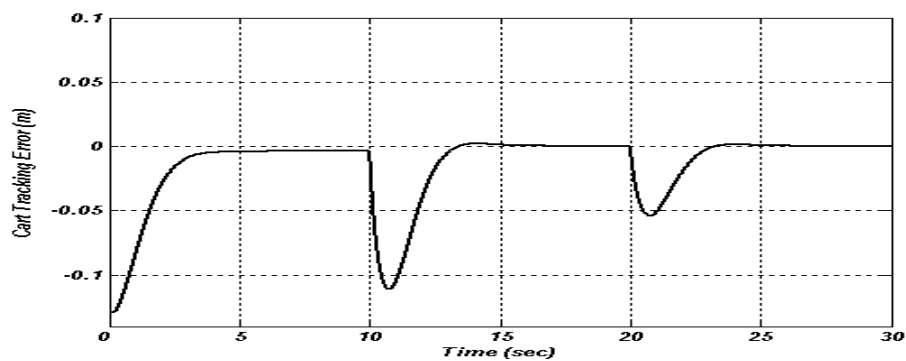


Figure (10): Variation of cart tracking error.

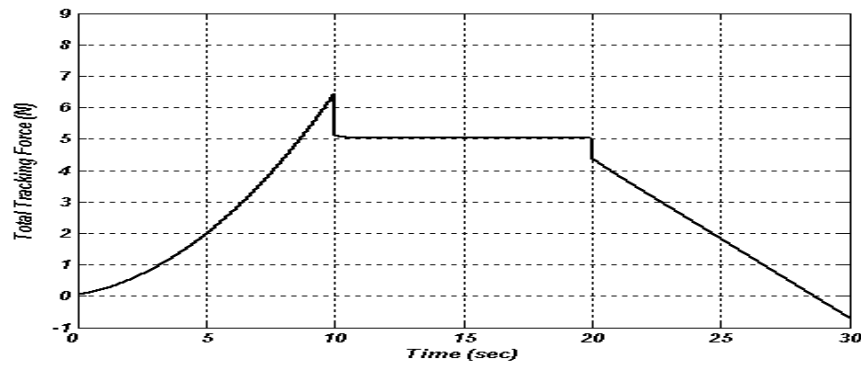
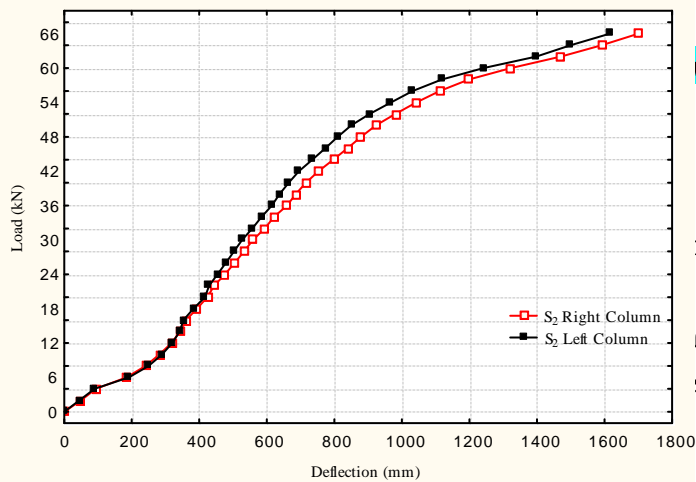


Figure (11): Total tracking force affecting the cart.

6. Conclusion

It is visible to utilize a jet force in stabilizing and vertically erecting an inverted pendulum cart system. An auxiliary pendulum attached to the inverted pendulum in a pendant position is needed in directing the stabilizing jet force in an open loop. The jet force plays as a positive stiffening parameter.

The system performs in a very good manner in tracking a specified trajectory. Despite the disturbances induced during tracking and the non-zero initial value, the inverted pendulum was kept stable with small transient oscillation about the vertical. The trajectory controller which is based on model reference/error driven scheme shows a very acceptable performance.



with inverted pendulum from simulation to remote
on and information technologies, Issue 3, Volume 1,

nukid Parinchkun, "Real time optimal control for
merican Journal of Applied Sciences, 6 (6), 1106-1115,

3. Usga, S. A. and Z. Adaptive integral back stepping motion control for inverted pendulum", World academy of science, engineering and technology, 29, 2007.
4. Nawawi S.W. et al, "Control of a two-wheels inverted pendulum mobile robot using full order sliding mode control", Proceeding of Int. conf. on man-machine systems, sept. 15-16, 2006, Langkawi, Malaysia.
5. Nawawi S.W. et al, "Real-time control of two-wheeled inverted pendulum mobile robot", World academy of science, engineering and technology, 39, 2008.
6. Mustafa Demirci, "control of a double inverted pendulum for non-linear systems.", Selcut, Applied Mathematics, Vol. 8, No. 1, pp. 27-43, 2007.
7. Futuwa, N. et al, "Development of vibration experiment", education materials for structural and soil dynamics, The 14th world conference on earth quick engineering, October 12-17, 2008, Beijing, China.
8. Baloh, M and Parent, M., "Modeling and model verification of an intelligent self-balancing two-wheeled vehicle for an autonomous urban transportation system", Conf. comp. intelligence, robotics and autonomous systems, Singapore, Dec., 15, 2003.
9. Yoshibiko Takahashi, et al, "Mechanical design and control of a robotic wheel-chair with inverse pendulum control", Transaction of the institute of measurement and control, Vol. 24, No. 5, 355-368, 2002.
10. Saifizul, A. A., et al, "Intelligent control for self-erecting inverted pendulum via adaptive Neuro-fuzzy inference system", American Journal of Applied Sciences, Vol. 3 (4), pp. 1795-1802, 2006.
11. Jin Seok Noh, et al, "Position control of a mobile inverted pendulum system using basis function network, Int. Journal of control, automation and systems, Vol. 8, No. 1, 2010.
12. Dario Maravall et al, "Hybrid fuzzy control of the inverted pendulum via vertical forces, Int. Journal of Intelligent systems, Vol. 20, 195-211, 2005.
13. Dare A. Wells, "Lagrangian Dynamics", McGraw-Hill Book Company, USA, 1967.
14. Hung V. Vu. and Esfandiari R. S., "Dynamic system, modeling and analysis", Irwin McGraw-Hill, USA. 1997.
15. John, J. Craig, "Introduction to robotics", mechanics and control, Addison-Wesley publishing company, 1989, second edition.
16. Slotine, J. E. and Li, W., "Applied non-linear control", Prentice-Hall, USA, 1991.